Cavity quantum electrodynamics with rare-earth ions in solids

Ding, D.

Chapter 3

Ion implantation and fiber connection

3.1 Ion implantation

We introduce ytterbium ions into devices with ring resonator structures using ion implantation techniques in collaboration with nuclear solid state group at the KU Leuven, Belgium. Yb^{2+} ions are first selected in the implanter to have only the isotope ^{174}Yb with a zero nuclear spin and are then implanted with an energy of 360 keV perpendicular to the device with a 200 nm thick SiO_2 top cladding. After the implantation Rutherford backscattering spectrometry (RBS) is performed on a reference sample and the resulting depth profiles for Yb, Si, and O that are obtained from numerical analysis using a computer program NDF [48] are shown in Fig. 3.1. The profile of implanted Yb ions can be well fitted by a Gaussian depth distribution with a mean value of 128 nm and a standard deviation of 37 nm (corresponding to a full width at half maximum (FWHM) of 86 nm). The implantation energy was carefully chosen not to introduce Yb ions into the Si_3N_4 core because implantation defects in SiO_2 and Si_3N_4 materials require different annealing temperatures to eliminate and their temperature ranges are incompatible with each other [49].

We studied the ion implantation processes by numerical simulations implemented in a computer program SRIM [50]. The accelerated ions are deflected and decelerated due to collisions with nuclei in the target material. To simulate this process, we inject 10^5 Yb ions with an initial energy of 360 keV into SiO_2 with a density of 2.2 g/cm^3 and record their stochastic trajectories. The overlapped trajectories of the ions are shown in Fig. 3.2(a) with both lateral and longitudinal (depth) distributions. Figure 3.2(b) shows the depth distribution of the ions. The depths are approximately Gaussian distributed with a center of 122 nm and a standard deviation of 27 nm (FWHM of 11 nm). Compared

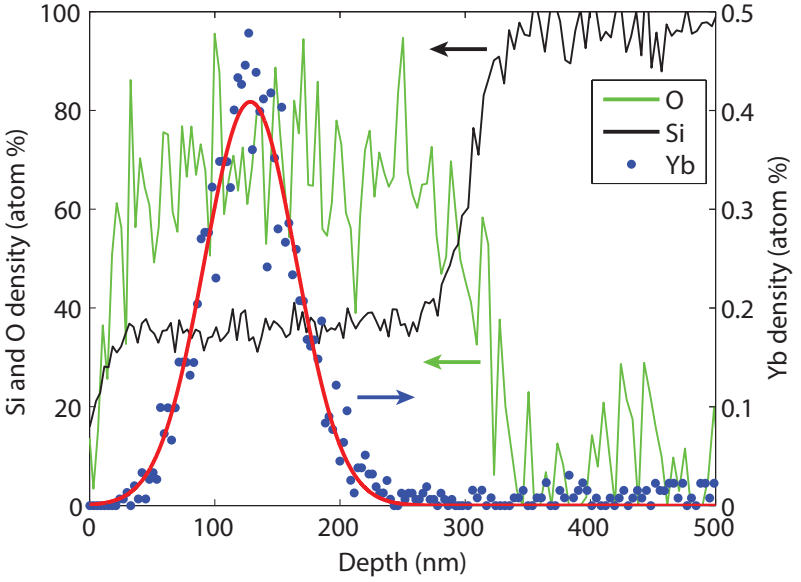

Figure 3.1: Depth profiles of Yb (blue dots), Si (black curve), and O (green curve) as determined by Rutherford backscattering spectrometry (RBS). Yb ions with an energy of 360 keV were implanted into a 310 nm thick, thermally grown, SiO_2 layer on a Si substrate. The RBS data were analyzed by using NDF [48] assuming a density of 2.2 g/cm^3 for the amorphous SiO_2. The depth profile of Yb is fitted by a Gaussian function (red curve) with a standard deviation of 37 nm (full width at half maximum of 86 nm) and with a center 128 nm underneath the surface.

with the experimental results of RBS, the simulation results of SRIM are lower by about 5% for the mean depth and by about 36% for the standard deviation. The accuracy of the SRIM simulation in the mean depth is believed to be better than 10% [51], although deviations by about 20% for the mean depth and by up to 50% for the standard deviation have been reported [52].

We compare our experimental data with literatures [49, 53, 54, 52, 55, 56, 57] and the results are shown in Fig. 3.3. Because erbium (Er) has an atomic number close to Yb (68 and 70), they share approximately the same properties in the implantation process and we compare the results of Er and Yb together. The data for the depth and standard deviation can be fitted by linear functions. Our experimental data are in good agreement with the values from literatures.

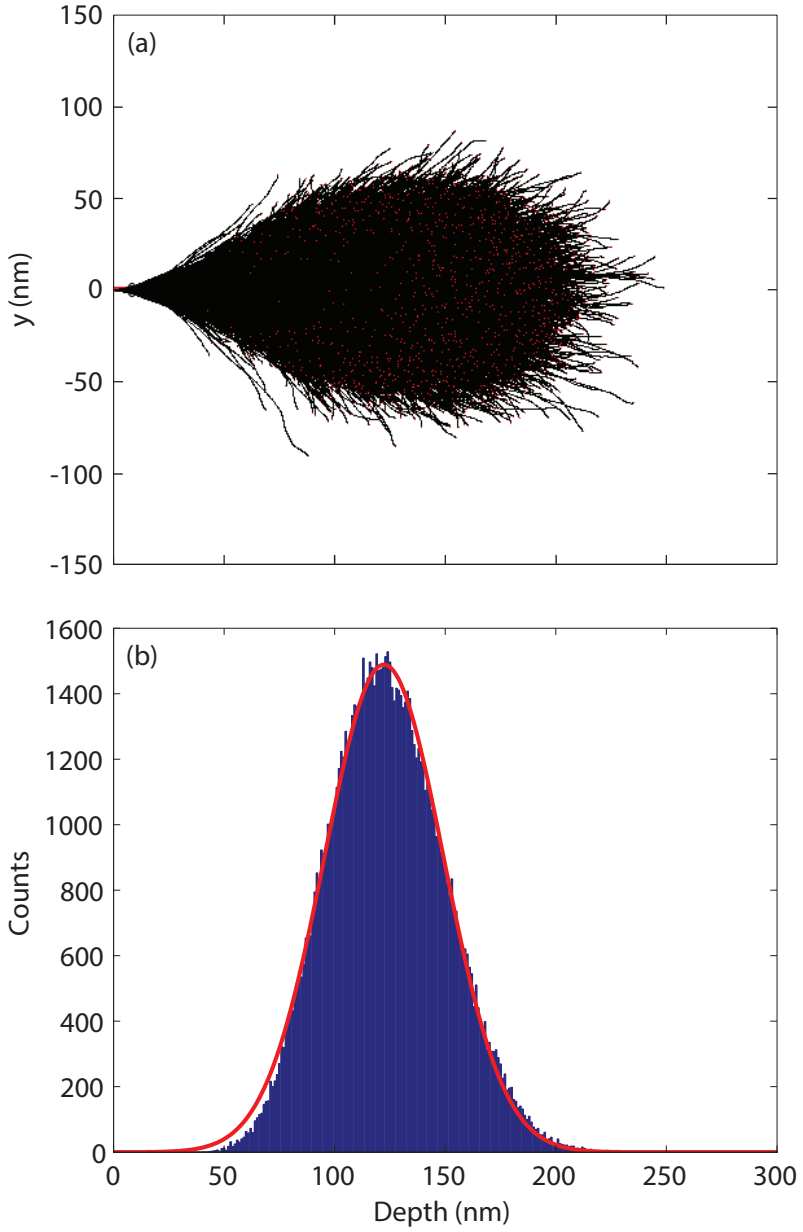

Figure 3.2: (a) Simulated trajectories of 10^5 Yb ions in SiO_2 projected in the xy-plane. The Yb ions with an initial energy of 360 keV are injected into SiO_2 at a coordinate of x (depth) $= 0$ and $y = 0$. The density of SiO_2 is assumed to be 2.2 g/cm^3. (b) Histogram (blue bars) of the Yb depths as shown in (a) with depth bins of 1 nm and a Gaussian fit (red curve) to the histogram. The fit results in a mean depth of about 122 nm and a standard deviation of about 27 nm (FWHM of 11 nm).

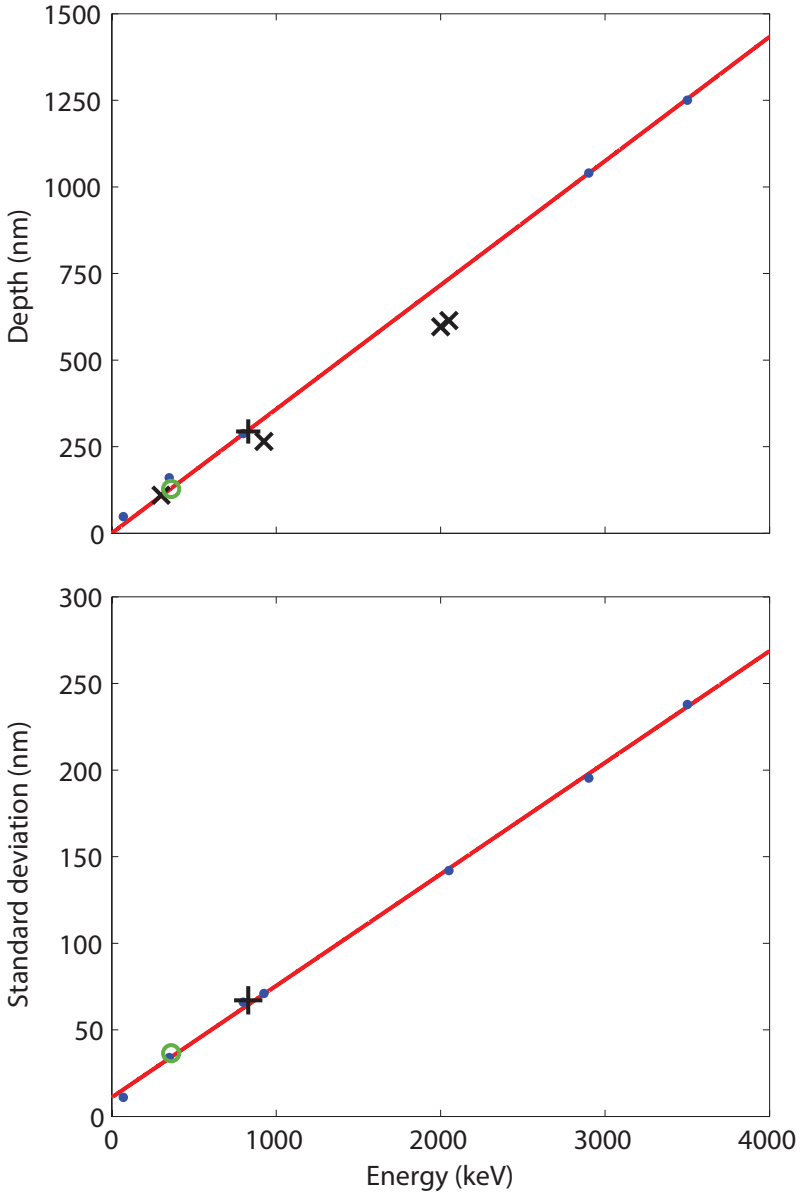

Figure 3.3: Experimental data of mean depths (a) and standard deviations (b) for erbium (blue dots and black crosses) and ytterbium (blue pluses and green circles) ions together with linear fits (red lines). The depth and standard deviation in our experiment determined by Rutherford backscattering spectrometry (RBS) are denoted by green circles, while other data points are adopted from Ref. [49, 53, 54, 52, 55, 56, 57]. In (a) three data points from Ref. [54, 55] denoted by black crosses apparently deviate from the trend of other data. Therefore the four data points from Ref. [54, 55] denoted by black crosses are not used in the fit. The fits result in two functions: [depth (nm)] = $0.36 \times$ [energy (keV)] and [standard deviation (nm)] = $0.064 \times$ [energy (keV)] + 11.0.

3.2 Fiber connection

In the research of integrated optics and solid-state quantum information processing, it is a routine task to couple light in and out of micro-structures such as waveguides and micro-cavities. Typically the structure has a well-defined Gaussian fundamental mode profile at a certain operating wavelength (a photonic crystal cavity is an exception though). To achieve high coupling efficiency, the two modes to be coupled to each other should match, i.e., on the transverse plane where they overlap, they should have the same beam size and radius of curvature. If the modal profile of the output beam from the structure is unimportant, e.g., if the output power is measured with a large-area photodetector, the collection mode matching becomes less critical—the collection optics just need to have an aperture larger than the output beam.

The most commonly used method to achieve good mode matching involves a high numerical aperture (NA) microscope objective or aspherical lens positioned close to the structure with a distance on the order of millimeter or less. Together with extra free-space optics, the mode matching can be optimized almost perfectly and the coupling efficiency readily exceeds 90%. When the structure is studied at low temperature, the microscope objective can be integrated in a cryostat and the sample with the structure is mounted on a cryogenic positioning stage. This method is ideal to study simple structures when pumping and collecting paths share the same microscope objective. However, complexity rises as more coupling ports on the structure, or more samples to be coupled to each other, because each port requires an independent microscope objective and positioning stage. This issue becomes more severe for low-temperature experiments, because of limited space in a cryostat and expensive cryogenic positioning stages.

In this section, we tackle this coupling scalability issue by positioning optical fibers to each port of the structure and fix the coupling permanently with UV curing optical adhesive at room temperature. We demonstrate that by carefully applying the optical adhesive and conducting cooling procedures, the coupling efficiency of the fiber-coupled structure remains the same at cryogenic temperature compared to room temperature after many cooling cycles. We shall discuss details of this technique and applications to waveguide-coupled ring resonators and to micro-pillar cavities.

3.2.1 General consideration

When a fiber-coupled sample is cooled down, the sample, fiber, and the substrate to which they are attached, shrink by different amounts. To avoid misalignment, there must be an adhesive spot between the fiber tip and the sample among other spots. This prevents using lensed fiber to achieve higher coupling

efficiency, but tapered fiber and fiber with a graded-index (GRIN) lens coupler are still options. Obviously the adhesive should have good optical properties such as high transmission at the operating wavelength and refractive index matching to the fiber and the structure. To overcome the misalignment caused by the thermal contraction of the adhesive itself, the adhesive spot at the coupling point should be as small as possible and be axisymmetric with respect to the fiber axis. The adhesive should also have low viscosity before cured such that one can finely tune the alignment with the adhesive applied. Besides, the curing time should be short otherwise the alignment drifts away. Other important requirements are low shrinkage, low stress, good adhesion to glass and high hardness after cured.

The small adhesive spot at the coupling point fixes the alignment, but it stands little forces. There must be another adhesive spot that fastens the fiber onto a substrate. For this adhesive spot, good mechanical properties at cryogenic temperature are paramount and there is no requirement for optical properties.

3.2.2 Technical details of coupling to waveguides

We will first describe the full technical details of fiber coupling to waveguides that are coupled to a ring resonator. The optical fiber that couples light into the waveguide is an ultra-high NA (UHNA) single-mode fiber from Thorlabs Inc. (part number UHNA3). For the operating wavelength of 980 nm of our devices, the fiber UHNA3 has a mode field diameter (MFD) of $\sim$2.5 μm and a NA of $\sim$0.35. Compared to normal single-mode fibers with a larger MFD, this UHNA fiber is coupled better to the mode of the waveguide that is typically around 1 μm in diameter. Without the ability to optimize the mode of the fiber, coupling efficiency of a fiber-coupled structure is usually lower than a well-optimized free-space-coupled structure. Nevertheless, for many applications, the coupling efficiency is still satisfactory. We shall focus on how to maintain the coupling efficiency while cooling down to liquid helium temperature.

An UHNA fiber is first stripped to remove polymer coating and then cleaved by a diamond cleaver. The resulting fiber has a flat tip and a stripping length of about 10 mm. It is then clamped on a high-precision xyz translation stage (NanoMax manual stage from Thorlabs Inc.) ready to be coupled to the input port of the structure. A cleaved multimode fiber (core diameter $\sim$50 μm) is clamped on another xyz translation stage to be coupled to the output port of the structure.

The sample is mounted on a substrate by using either cryogenic silver epoxy or Stycast epoxy (from Lakeshore Cryogenics Inc.) which ensures good thermal conductivity and mechanical strength at low temperature. The substrate for the sample is also the one where the coupling fibers are eventually attached. It

can be simply a large piece of silicon wafer, fused silica, or specially designed copper plate. The advantage of using silicon wafer as substrate lies in the fact that it has both low thermal expansion coefficient and high thermal conductivity. The substrate with the sample is mounted on a tilt and rotation stage next to the translation stages on which the two fibers are clamped. The fibers are parallel to the substrate in the case of coupling to waveguides.

A microscope is used to monitor and to guide the alignment between the structure and the fibers. Once the system is pre-aligned by imaging, light from a narrow-linewidth laser (DL Pro, Toptica Photonics AG) is launched into the UHNA fiber and transmission through the multimode fiber is measured. The laser frequency is scanned in a small spectral range such that resonances in the transmission spectrum can be observed when the laser frequency is on resonance with the ring resonator. The system is finely aligned by optimizing the resonant transmission amplitude.

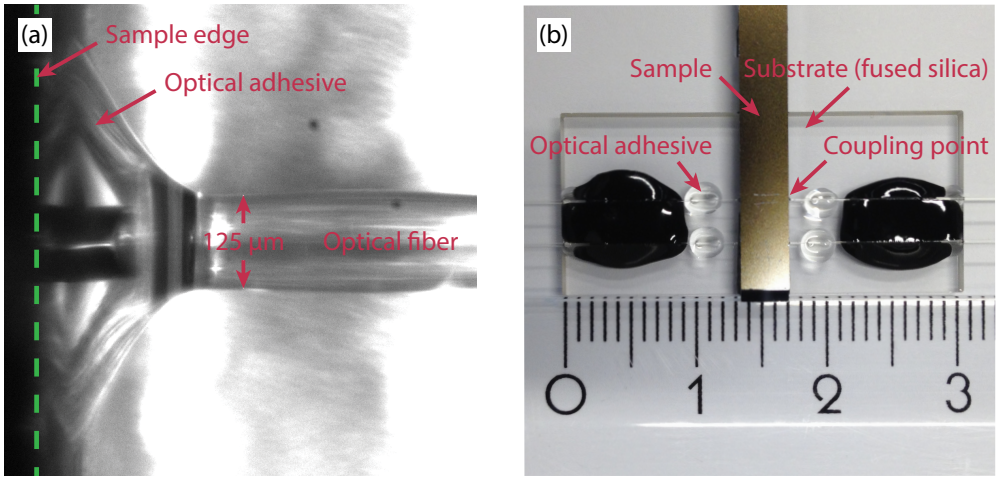

Figure 3.4: (a) Microscopic image of the coupling point showing a stripped and cleaved optical fiber with a diameter of 125 μm coupled to a waveguide. The coupling is fixed by UV curing optical adhesive. (b) Photograph of a sample with waveguide structures coupled to four optical fibers on a fused silica substrate.

After the system is aligned, the UHNA fiber is released from the clamp and dipped into a small droplet (diameter ~0.5 mm, generated at the tip of a syringe needle) of UV curing optical adhesive (NOA61, Norland Products Inc.). Once the fiber is retracted from the adhesive droplet, a tiny ball-shaped adhesive is attached at the fiber tip. The fiber is then clamped back onto the translation stage and the system is re-aligned according to the previous procedures. When the ball-like adhesive on the fiber tip touches the sample, surface tension pulls the adhesive to the coupling point and renders the coupling area well surrounded by the adhesive. Subsequently, the adhesive is cured

by power UV LEDs at 365 nm wavelength in 10 min. A microscopic image of the coupling point is shown in Fig. 3.4(a). The small and axisymmetric adhesive spot at the coupling point ensures negligible misalignment caused by the thermal contraction of the adhesive itself while cooled down to cryogenic temperature.

Followed by the curing of the adhesive at the coupling point, a large droplet of the same adhesive is applied and UV cured on the fiber and the substrate with about 5 mm away from the coupling point to strengthen the fiber connection. A photograph of a fiber-coupled sample is shown in Fig. 3.4(b). The diameter of this adhesive spot is about 3 mm on the substrate. It is important to limit the size of this adhesive spot because for a large volume of cured optical adhesive (1) it tends to crack during cooling and (2) the stress due to different thermal contraction between the adhesive and the substrate is also relatively large which leads to release of contact. It has been tested that this optical adhesive spot is sufficiently strong to maintain good coupling efficiency upon cooling cycles for normal applications. More fibers can be coupled to the structure by repeating the above procedures.

3.2.3 Technical details of coupling to micro-pillar cavities

As to the fiber coupling to micro-pillar cavities, since the structure is perpendicular to the sample surfaces, there is a small opening (diameter $\sim$2 mm) on the substrate to access the output port of the structure. The coupling fiber first passes through a ceramic ferrule which is embedded in a large copper ferrule. The length of the fiber that protrudes out of the ceramic ferrule is calculated such that once the fiber tip contacts the structure the distance from the substrate to the copper ferrule is about 1 mm. The relative positions of the fiber and the two ferrules can be fixed by Stycast epoxy. The copper ferrule is then clamped onto a xyz translation stage for alignment. The sample is illuminated by laser light at 1060 nm wavelength through the UHNA fiber and a microscope is used to collect transmitted light from the opposite side of the sample. The 1060 nm laser light is in the transmission band of the sample made of GaAs and AlGaAs. Microscopic images of the micro-pillar sample under back-illumination of 1060 nm laser light through the UHNA fiber are shown in Figs. 3.5(a) and 3.5(b). Once the system is pre-aligned by imaging, light from a narrow-linewidth laser is launched into the UHNA fiber and transmission through the structure is measured by a photodetector at the opposite side of the sample. Fine alignment is achieved by optimizing the resonant transmission amplitude. A microscopic image of the micro-pillar sample under back-illumination of resonant laser light through the UHNA fiber is shown in Fig. 3.5(c).

Adhesion of the coupling point is the same as the fiber coupling to waveg-

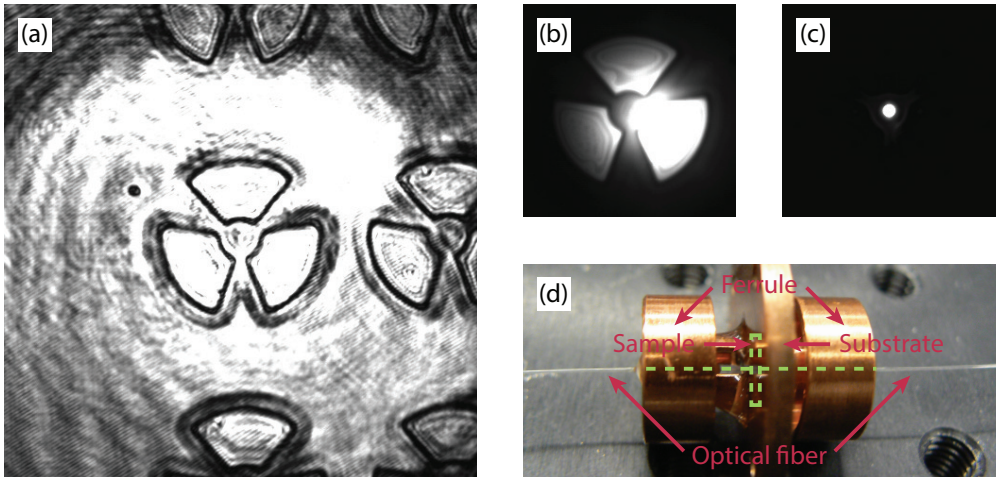

Figure 3.5: (a) and (b) Microscopic images of a micro-pillar sample under back-illumination of 1060 nm laser light through an ultra-high numerical aperture (UHNA) fiber. The distributed Bragg reflectors (DBR) made of alternating layers of GaAs and AlGaAs on the sample are transparent to the 1060 nm laser light. In (a) the fiber is relatively distant from the sample and therefore a large area is illuminated showing a part of the micro-pillar cavity array on the sample. Each micro-pillar cavity is surrounded by three etched trenches from the edges of which oxidation starts on an AlAs layer to form a tapered aperture. In (b) the fiber is further positioned closer to the sample and aligned with the central micro-pillar cavity as shown in (a). (c) Microscopic images of the sample under back-illumination of narrow-linewidth laser light through the fiber with the laser frequency on resonance with the cavity fundamental mode. Only the light that is coupled to the cavity mode is transmitted and the uncoupled light is reflected by the DBR. The fiber is finely aligned with the cavity mode by maximizing the resonance transmission of the laser light. (d) Photograph of a micro-pillar sample mounted on a copper substrate coupled to two optical fibers at opposite sides. These couplings are fixed by UV curing optical adhesive.

uides. Eventually the fiber is fixed onto the substrate by applying and curing optical adhesive between the copper ferrule and the substrate. The output coupling fiber can be aligned to the output port of the structure by optimizing the resonance transmission through the input-output fibers. Adhesion procedures are exactly the same as the input coupling fiber.

3.2.4 Cooling procedures

If the substrate is made of copper or silicon with good thermal conductivity, the substrate can be attached to the cold plate of the cryostat. On the other hand, if the substrate is made of fused silica with poor thermal conductivity, the sample surface can be attached to the cold plate. A thin layer of cryogenic varnish is preferable in between the cold plate and the substrate or the sample

for better contact. Mechanical clamping is usually required to strengthen the contact. All the fibers pass through the cryostat via reusable fiber feedthroughs [58].

Cooling rate should be low to protect the adhesive spots. In practice, the cooling rate is kept as low as 20 mK/s. This means that it takes about four hours to cool down from room temperature to liquid helium temperature. Our fiber-coupled waveguide-ring-resonator sample has been tested for eight cooling cycles between room temperature and liquid helium temperature without appreciable deterioration of coupling efficiency.